

Thermomigration of Liquid Droplets in Salt

T. R. Anthony
H. E. Cline

General Electric Research and Development Center
Schenectady, New York

ABSTRACT

The salt mine burial of fission waste products resulting from the reprocessing of spent fuel elements is now planned as a permanent means of disposal of these highly radioactive wastes. Although salt mine burial is apparently the best method of disposal, the vigorous self-heating of these waste products leads to some potential problems. Natural salt formations regularly contain small brine inclusions which will migrate up the thermal gradients generated by the self-heating of the waste products. The resulting inflow of water into the nuclear waste crypts is undesirable because water vapor may accelerate waste container corrosion and/or lead to fission product contamination of currently unused sections of the salt mine. In addition, contaminated vapor-liquid biphasic droplets generated on the walls of the nuclear waste crypt are capable of dispersing fission products throughout the salt formation since these unusual inclusions migrate down thermal gradients, in contrast to the normal thermomigration of simple gas or liquid droplets up thermal gradients in salt. By considering viscous gas flow, vapor diffusion, liquid diffusion, evaporation and condensation, and liquid currents driven by surface tension gradients, the odd thermomigration behavior of the vapor-liquid droplets observed in the present investigation is explained. It is concluded that a modest dispersal of radioactive wastes may occur in the salt formation. However, because of droplet trapping by the grain boundaries in the salt, the escape of radioactivity to the outside environment is unlikely even on a geological time scale.

INTRODUCTION

As a permanent solution to the disposal of radioactive nuclear waste products it has been proposed that such wastes be permanently stored in abandoned salt mines.⁽¹⁻⁸⁾ Because of the seismic stability of salt formations and the

plasticity of salt under pressure, the possible release of radioactive wastes by earth movement or strata fracture would be minimized in this type of mine.

The initial self-heating of the high-level wastes, however, leads in principle, to some potential dispersal problems that we will concern ourselves with in this paper. Salt formations regularly contain about 0.4 atomic percent water in the form of small liquid-brine inclusions with typical diameters of a few hundred microns.⁽⁹⁾ Because of the self-heating of the radioactive wastes, temperatures up to 300°C can be reached in the nuclear waste crypts in a salt mine.⁽⁷⁻¹¹⁾ Such temperatures would generate temperature gradients extending radially away from the crypts into the surrounding salt formation. These temperature gradients can cause the thermomigration of brine inclusions in the salt formation towards and eventually into the waste product crypts. The resulting release of water vapor into the salt mine is undesirable because water vapor may accelerate waste container corrosion and/or cause dispersion of fission products into currently unused sections of the salt mine.⁽⁹⁾

When a brine droplet impinges on the crypt wall, not all of the liquid in the droplet is lost to the surrounding atmosphere. On the contrary, as water evaporates from the saturated brine, precipitation of salt generally reseals the inclusion and prevents further water evaporation. The resealed droplet now contains both liquid brine and a gas bubble. These biphasic vapor-liquid inclusions have one outstanding and important characteristic. In a temperature gradient, vapor-liquid inclusions migrate *down the temperature gradient* toward lower temperatures⁽¹²⁻¹⁵⁾ in contrast to the usual thermomigration of simple liquid or gas inclusions *up a temperature gradient*.

If the vapor-liquid droplets become contaminated with radioactive wastes as they are generated on the walls of the crypt, the containment integrity of the crypt may suffer

when the vapor-liquid droplets migrate down the temperature gradient away from the crypt. Any degree of dispersal of radioactivity in the surrounding salt formation should be avoided since such dispersal would greatly increase the difficulty of exhuming the high-level radioactive wastes buried in the mine should the need ever arise in the future.

In order to predict the possible degree of radioactive waste dispersal in the salt strata surrounding the burial crypt, we have measured the velocity of vapor-liquid droplets in a temperature gradient as a function of their size and relative proportions of vapor and liquid. By considering the conservation of salt and water, gaseous diffusion, viscous gas flow, liquid currents generated by surface tension gradients, liquid diffusion and interface kinetics, a model of the migration process is derived which adequately describes our experimental observations of the thermomigration of biphasic vapor-liquid inclusions.

EXPERIMENTAL

Sample preparation

A single crystal of KCl $3 \times 3 \times 10$ mm with less than 30 ppm of impurities was obtained from the Harshaw Chemical Co. A cylinder of brine was produced in the salt crystal by drilling a 0.3 mm diameter hole in the crystal, filling the hole with deionized water and sealing with wax to prevent evaporation. A thermal gradient of $20^\circ\text{C}/\text{cm}$ was applied along the length of the salt crystal for one week. During the first few days, the brine cylinder simultaneously migrated and disintegrated into a myriad of small brine droplets with a size range of 2–150 microns.⁽¹⁶⁾ The isolated brine droplets continued to migrate up to the temperature gradient until they came to the hot end of the crystal. There at the crystal surface, the brine in the liquid droplets partially evaporated until salt precipitation generated by the evaporation resealed the droplets. The resulting biphasic vapor-liquid droplets then turned around and migrated down the temperature gradient back into the crystal.

Droplet velocity and droplet break-up

The velocities of a number of vapor-liquid droplets in a thermal gradient of $3^\circ\text{C}/\text{cm}$ were measured from the time series of photomicrographs shown in Fig. 1. The velocities of the various droplets of Figure 1 that migrated as a single unit (droplets B, D, E, F, G, H, and L) are shown in Table I along with the vapor volume fraction and the dimensions of the droplets. Table I indicates that droplets with a greater fractional gas content and larger size migrate more rapidly than droplets with a lower fractional gas content and a smaller size.

Attempts to measure the velocities of specific droplets at different temperatures and in different temperature

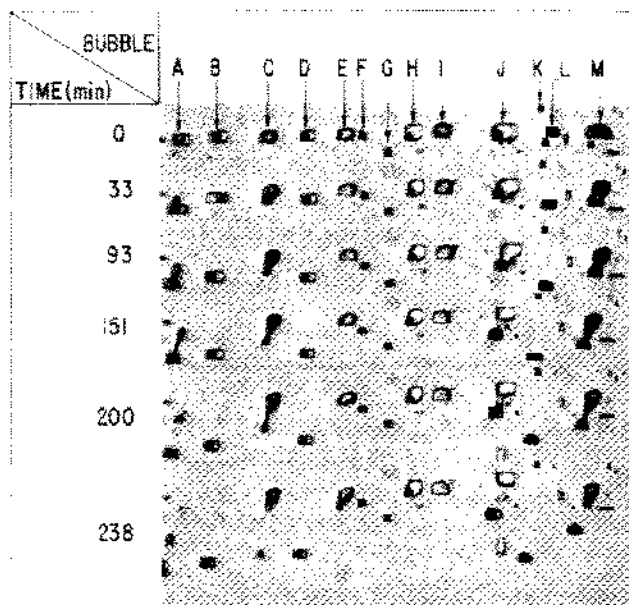


Figure 1. The migration of a number of vapor-liquid (air- H_2O) droplets in a thermal gradient of $3^\circ\text{C}/\text{cm}$ in KCl. The dark phase is the gas phase while the light phase is the liquid phase. The thermal gradient is in a vertical direction with higher temperatures upwards and lower temperatures toward the bottom of the photograph. The positions of the droplets which were initially on the same starting line are shown at times of 0, 33, 93, 151, 200, and 238 minutes. The very small liquid droplets such as those just to the right of bubbles I and M do not move during the experiment because of an interface kinetic barrier. (16, 31)

TABLE I

The measured velocities, sizes, and relative proportions of vapor and liquid phases of the various vapor-liquid biphasic droplets of Figure 1.

Droplet	Velocity (cm/sec)	X (N)	L (N)	Vapor Bubble Diameter (N)	Fractional Gas Content of Droplet
1	4.3×10^{-7}	8	8	8	0.52
2	3.5×10^{-7}	15	14	14	0.46
3	3.5×10^{-7}	15	12	9	0.14
4	3.1×10^{-7}	18	12	10	0.13
5	3.0×10^{-7}	10	9	9	0.42
6	2.9×10^{-7}	17	9	12	0.35
7	1.2×10^{-7}	8	9	8	0.47
8	1.1×10^{-7}	8	9	8	0.47
9	3.2×10^{-8}	15	12	10	0.19
10	negligible	18	18	9	0.07
11	negligible	8	8	6	0.22

Average Velocity 2.5×10^{-7}

Average Gas Content 0.35

gradients were frustrated by the general tendency of vapor-liquid droplets to split apart when the temperature or temperature gradient was changed. For example, for the temperature of 40°C and the temperature gradient of $3^\circ\text{C}/\text{cm}$ of Figure 1, vapor-liquid droplets A, C, J, and M eventually divided. The division of droplet J was particu-

larly interesting. The displacement versus time of the various parts of this droplet are shown in Figure 2. Initially, droplet J was a large vapor-liquid droplet containing a relatively high proportion of liquid. On application of the $3^\circ\text{C}/\text{cm}$ temperature gradient to the crystal, droplet J began to divide itself into two progeny: a vapor-liquid droplet which began to migrate down the temperature gradient and a simple liquid droplet which commenced to migrate up the temperature gradient. The liquid neck connecting the two offspring (see Fig. 1 at 151 and 200 minutes) restrained both the simple liquid droplet and the biphasic vapor-liquid droplet from going their respective ways. The restraining force of this liquid neck is equal to the solid-liquid surface tension γ_{SL} times the perimeter of the liquid neck.^(17, 18) As the liquid neck became thinner and thinner, the force holding the two droplets together decreased until this connecting neck broke. The separated droplets then continued on their separate ways up and down the thermal gradient, respectively (Fig. 1 at 238 minutes).

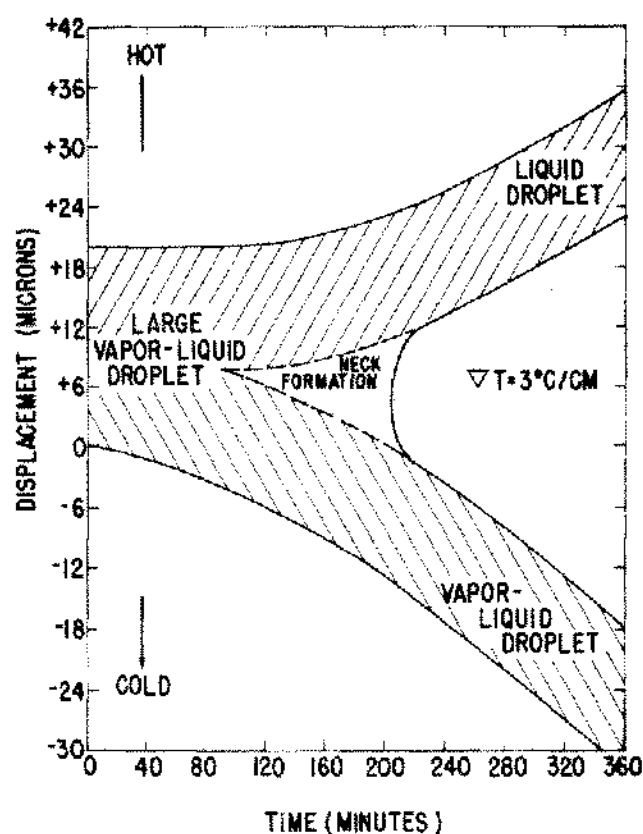


Figure 2. The breakup of bubble J of Figure 1 into a simple liquid droplet and a vapor-liquid droplet. The liquid droplet migrates towards the hot side while the vapor-liquid droplet moves towards the cold side of the sample. Both offspring droplets are temporarily restrained from going their separate ways by the surface tension of the liquid neck holding the offspring droplets together.

DISCUSSION

The physical processes involved in the thermomigration of vapor-liquid droplets

Figure 3 is a schematic diagram of a biphasic vapor-liquid droplet migrating down a temperature gradient where the gas bubble has been approximated as a cube. On the hot face of the droplet, water evaporates from the brine film into the vapor phase. The resulting salt supersaturation in the brine film causes salt to precipitate on the hot face of the droplet. The evaporated water is then transported through the gas phase to the cold side of the droplet where it condenses on the cold brine film. There, the condensed water dilutes the brine below the saturation level and thus causes dissolution of salt from the cold side of the droplet. This simultaneous dissolution of salt on the cold face and deposition of salt on the hot face of the droplet causes the thermomigration of the droplet down the temperature gradient toward lower temperatures.

In order that water is continually available for evaporation from the hot face, a counterflow of water must occur in the liquid-brine film from the cold to the hot face of the droplet. This counterflow of liquid is generated by a vapor-liquid surface tension gradient between the hot and cold faces of the droplet. The vapor-liquid surface tension of

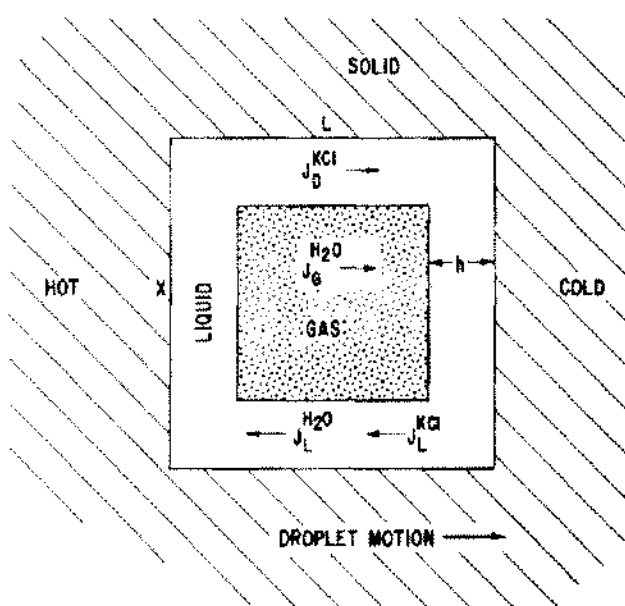


Figure 3(a). A schematic diagram of a biphasic vapor-liquid droplet migrating down a temperature gradient in a solid. The cyclic flow of water around the droplet is accomplished by a flux of water $J_{\text{H}_2\text{O}}^{\text{G}}$ through the vapor phase and a counter current of water $J_{\text{H}_2\text{O}}^{\text{L}}$ in the liquid phase. The net flow of salt through the droplet which gives rise to the thermomigration of the droplet is the sum of the counter fluxes of salt in the liquid caused by liquid flow $J_{\text{KCl}}^{\text{L}}$ and diffusion $J_{\text{KCl}}^{\text{D}}$.

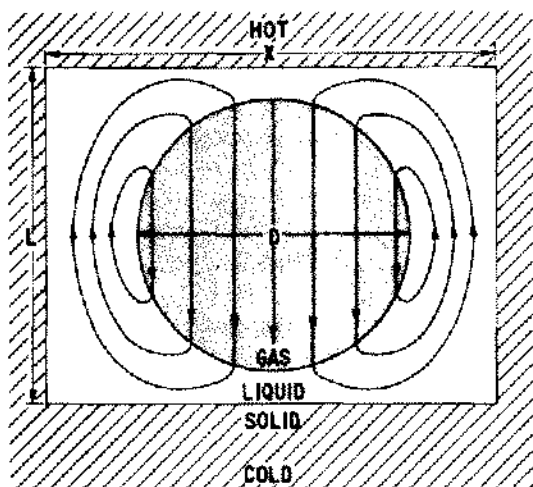


Figure 3(b). Water flow lines in a vapor-liquid droplet migrating down a thermal gradient toward lower temperatures. In those vapor-liquid droplets which contain only a modest gas fractional content, the gas phase is spherical as shown in the figure. For vapor-liquid droplets containing a large fractional gas content, the thin film of liquid on the solid interface of the droplet gives the gas bubble a cubic shape as shown in Figure 3(a).

the concentrated brine solution on the hot face is higher than the surface tension of the pure water condensed on the surface of the brine on the cold face since salt increases the vapor-liquid surface tension of water. The resulting surface tension gradient is equivalent to a shear stress on the surface of the liquid directed towards the hot side of the droplet and causes a flow of water from the cold to the hot side, completing the water cycle (see Fig. 4).

Water and salt conservation equations

The thermomigration of the vapor-liquid droplet can be described by two mass conservation equations for water and salt, respectively. If $J_{H_2O}^G$ and $J_{H_2O}^L$ are the fluxes (in moles/cm²-sec) of water through the vapor and liquid phases of the droplet, respectively, and are expressed with respect to the coordinates of the center of the moving droplet, then

$$J_{H_2O}^G A_G - J_{H_2O}^L A_L = 0: \text{Conservation of } H_2O \quad (1)$$

since no water is left behind by the migrating vapor-liquid droplet. A_G and A_L are the average cross-sectional areas perpendicular to the thermal gradient of the gas and liquid phases of the droplet, respectively.

Similarly, a net flux of salt equal to $V C_S^{KCl}$, where V is the vapor-liquid droplet velocity and C_S^{KCl} is the concentration of salt in solid salt, must pass through the droplet in order that the droplet migrate with a velocity V . This net flux of salt from the cold to the hot face results from the competition between the salt flux J_{KCl}^L generated by the flow of liquid brine from the cold to the hot face (see Figs. 3 and 4) and the opposing diffusion flux J_{KCl}^G

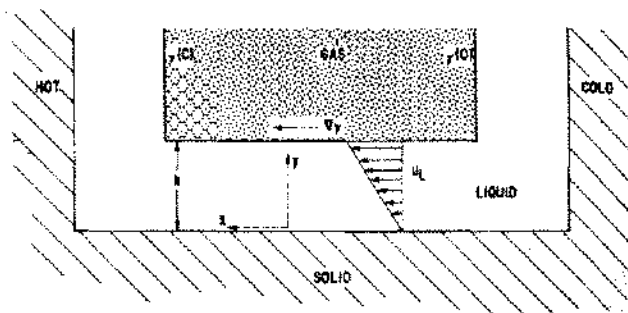


Figure 4. A schematic diagram of the liquid current J_L in a vapor-liquid droplet generated by the liquid-vapor surface tension gradient between the hot and cold droplet faces. U_L is the velocity of an element of liquid and increases from zero at the solid-liquid interface to its maximum value on the vapor-liquid interface. The surface tension gradient is caused by the difference of brine concentration at the liquid surface between the hot and cold faces of the droplet.

of salt from the hot to the cold face in the liquid caused by the salt concentration drop across the droplet

$$(J_L^{KCl} - J_D^{KCl}) A_L = (A_G + A_L) V C_S^{KCl}: \text{Conservation of salt} \quad (2)$$

The flux of KCl , J_L^{KCl} , caused by the liquid flow is simply related to the water flow $J_L^{H_2O}$ by,

$$J_L^{KCl} = \frac{C_L^{KCl}}{C_L^{H_2O}} J_L^{H_2O} \quad (3)$$

The velocity V of the biphasic vapor-liquid droplet can be obtained by combining Equations (1), (2), and (3) once the expressions for the individual fluxes J have been derived.

Flux of water through the gas $J_{H_2O}^G$

Vapor phase contains only H_2O vapor. When the gas phase contains only water vapor, the transport of water through the vapor phase from the hot to the cold side of the droplet occurs by viscous gas flow down the pressure gradient across the droplet. If ΔP is the pressure gradient across the droplet generated by the change of the vapor pressure of water with temperature, a modified Poiseuille Law equation shows that the flux of water vapor is:

$$J_{H_2O}^G = C_G^{H_2O} \frac{\Delta P (x - 2h)^2}{25 \eta_{H_2O}^G (L - 2h)} \quad (4)$$

where

$$\Delta P = \frac{\partial P_{H_2O}^G}{\partial T} \nabla T_G (L - 2h), \nabla T_G$$

is the temperature gradient in the gas, $\eta_{H_2O}^G$ is the viscosity of water vapor and L , X , and h are the droplet dimensions shown in Figure 3. Inserting values of the various constants in Table II for the conditions of the experiment, we find that $J_{H_2O}^G = 2.6 \times 10^{-4}$ moles/cm²-sec.

TABLE II

The various physical constants associated with the KCl-H₂O and the NaCl-H₂O systems at a temperature of 40°C. These constants can be found in the various references listed at the end of this article.

Symbol	KCl	NaCl	H ₂ O
C_L	5.1×10^{-3} moles/cm ³	6.0×10^{-3} moles/cm ³	5.56×10^{-2} moles/cm ³
$\frac{\partial C_L}{\partial T}$	$3.9 \times 10^{-5} \frac{\text{moles}}{\text{cm}^3 \cdot ^\circ\text{K}}$	$9.9 \times 10^{-5} \frac{\text{moles}}{\text{cm}^3 \cdot ^\circ\text{K}}$	---
C_s	2.66×10^{-2} moles/cm ³	3.72×10^{-2} moles/cm ³	---
C_G	---	---	2.87×10^{-6} moles/cm ³
$\frac{\partial C_G}{\partial T}$	---	---	$1.45 \times 10^{-7} \frac{\text{moles}}{\text{cm}^3 \cdot ^\circ\text{K}}$
P_G	---	---	7.45×10^4 dynes/cm ²
$\frac{\partial P_G}{\partial T}$	---	---	$4.05 \times 10^3 \frac{\text{dynes}}{\text{cm}^2 \cdot ^\circ\text{K}}$
n_L	---	---	6.6×10^{-3} gm/cm-sec
n_G	---	---	1.2×10^{-4} gm/cm-sec
D_G	---	---	0.239 cm ² /sec
D_L	2.165×10^{-5} cm ² /sec	1.47×10^{-5} cm ² /sec	---
$\frac{\partial \gamma}{\partial C}$	$1.4 \frac{\text{erg-liter}}{\text{cm}^2 \cdot \text{mole}}$	$1.64 \frac{\text{ergs-liter}}{\text{cm}^2 \cdot \text{mole}}$	---
$\frac{\partial \gamma}{\partial T}$	---	---	$0.167 \frac{\text{ergs}}{\text{cm}^2 \cdot ^\circ\text{K}}$
α	$1.35 \times 10^{-3} / ^\circ\text{C}$	---	---
$\beta: (V' = \beta \nabla T_s)$	4.8×10^{-8} cm ² /sec-°K	5.9×10^{-9} cm ² /sec-°K	---
α (foreign gas): $V = \alpha \nabla T_s$	1.6×10^{-7} cm ² /sec-°K	1.51×10^{-7} cm ² /sec-°K	---
α (no foreign gas): $V = \alpha \nabla T_s$	1.53×10^{-4} cm ² /sec-°K	1.45×10^{-4} cm ² /sec-°K	---

Miscellaneous Constants

$\{H_2O \text{ (in natural salt)}\}$	$= 1.08 \times 10^{-4}$ moles/cm ³ of salt
∇T_{earth}	$= 2 \times 10^{-4}$ °C/cm
RT	$= (8.31 \times 10^7 \frac{\text{ergs} \cdot ^\circ\text{K}}{\text{mole}}) (313^\circ\text{K})$
$\nabla T_L \approx \frac{3}{2} \nabla T_s$	$= 4.5^\circ\text{C/cm}$
$\nabla T_G \approx \frac{3}{2} \nabla T_s$	$= 4.5^\circ\text{C/cm}$

For relatively large values of $J_{H_2O}^0$, one must be sure that the evaporation and condensation rate of water at the liquid-vapor interface does not limit the flow of H₂O across the vapor phase of the droplet. The evaporation and condensation rate R of a pure gas over its own liquid is given by

$$R = \sqrt{\frac{P(1-z)}{2\pi mkT}}$$

where P is the vapor pressure of the gas, m is the mass of a gas molecule, kT is Boltzmann's constant times the abso-

lute temperature and z is an accommodation coefficient. For water vapor at 40°C, $R = 2.2 \times 10^{-2}$ moles/cm²-sec assuming that $z = 1/2$. Since the evaporation-condensation process is two orders of magnitude faster than the viscous gas flow process, evaporation-condensation will not control the flux of water across the vapor phase of the droplet for the temperatures and temperature gradients of our experiment. Vapor-liquid biphasic droplets in which the gas phase contains only the vapor of the liquid can be easily produced by temporarily vaporizing⁽¹⁹⁻²²⁾ or freezing⁽²³⁾ liquid inclusions in solids.

Vapor phase contains a foreign gas. When the vapor phase contains an appreciable amount of foreign gas, water vapor transport through the gas phase is accomplished by a diffusion process from the hot to the cold side of the droplet. If the Soret effect which is very small in gases⁽²⁴⁾ is ignored, the flux of water $J_G^{H_2O}$ in this case is,⁽²⁵⁾

$$J_G^{H_2O} = D_G^{H_2O} \frac{\partial C_G^{H_2O}}{\partial T} \nabla T_G \quad (5)$$

where $D_G^{H_2O}$ is the diffusivity of water in the foreign gas and $C_G^{H_2O}$ is the concentration of water in the gas phase. For the conditions of our experiment, $J_G^{H_2O} = 1.6 \times 10^{-7}$ moles/cm²-sec.

The counter current of liquid brine J_L

The continuous cyclic flow of water back and forth across the droplet may be limited in some cases by the counterflow rate of liquid brine from the cold to the hot side of the droplet. This flow of liquid is caused by the liquid-vapor surface tension gradient $\Delta_x \gamma$ generated by the difference in salt concentration in the brine between the hot and cold faces of the droplet. Let U be the velocity of a small volume of liquid parallel to the facet plane of the droplet (the x direction) and y be the position coordinate perpendicular to the direction of flow (see Fig. 4). Then the Navier-Stokes equation

$$n_L^{H_2O} \frac{\partial^2 U}{\partial y^2} = 0$$

describing this fluid flow can be solved to give

$$n_L^{H_2O} U = y \nabla_x \gamma \quad (6)$$

where $n_L^{H_2O}$ is the viscosity of brine and where the boundary conditions of a zero liquid velocity at the solid-liquid interface and a surface shear stress of $\Delta_x \gamma$ at vapor-liquid interface have been used.^(26, 27) The average flow of water per unit areas is then

$$J_L^{H_2O} = C_L^{H_2O} \frac{\int_0^h U dy}{h} = \frac{(\nabla \gamma_x) h C_L^{H_2O}}{2n_L^{H_2O}} \quad (7)$$

The surface tension gradient $\Delta_x \gamma$ is given by the change of surface tension with salt concentration

$\frac{\partial \gamma}{\partial C}$ times the change of salt concentration ΔC between the hot and cold faces divided by the length of the droplet, $L-2h$, parallel to the thermal gradient:

$$\nabla_x \gamma = \frac{\partial \gamma}{\partial C} \frac{C}{L-2h}$$

The concentration change ΔC is equal to the total salt solubility C_L^{KCl} in brine at the temperature of the droplet

since the condensing water on the surface of the cold face of the droplet is pure water and the brine on the hot face of the droplet is saturated.⁽²⁸⁾ Equation (7) becomes then,

$$J_L^{H_2O} = C_L^{H_2O} \frac{C_L^{KCl}}{2n_L^{H_2O}} \frac{\partial \gamma}{\partial C} \frac{h}{(L-2h)} \quad (8)$$

Substituting typical values of $L = 15 \times 10^{-4}$ cm and $h = 1 \times 10^{-4}$ cm and the constants in Table II, we find that $J_L^{H_2O} = 2.43$ moles of H_2O /cm²-sec. Since $J_L^{H_2O}$ caused by chemocapillarity effects is substantially greater than either diffusional flow or viscous gas flow of H_2O through the vapor phase of the droplet, it will not be the process controlling the rate of the cyclic flow of water around the vapor-liquid droplet. Consequently, the observed vapor-liquid droplet velocity will not be determined by this chemocapillarity hydrodynamic process.

In summary then, the rate of cyclic flow of H_2O between the hot and cold faces of the droplet will be controlled by diffusion in the vapor when the vapor contains a foreign gas and by viscous gas flow when the gas phase contains only H_2O vapor.

Diffusion flux of salt in the liquid

Of the fluxes in the basic conservation Equations (1) and (2), only the diffusion flux J_D^{KCl} of salt in the liquid has not been discussed. In a previous paper⁽¹⁶⁾, we showed that this flux will be given by

$$J_D^{KCl} = C_L^{KCl} D_L^{KCl} \left[\left(\frac{\partial \ln C_L^{KCl}}{\partial T} + \sigma \right) \nabla T_L + \frac{K}{LKT} \right] \quad (9)$$

where D_L^{KCl} is the diffusion coefficient of KCl in brine, σ is the Soret coefficient of KCl in brine, ΔT_L is the thermal gradient in the brine, and K is the interface kinetic potential^(16, 29-31) for the KCl- H_2O system. Note that in Equation (9), a plus sign in place of the minus sign in reference 16 is in front of the interface kinetic potential. This effective enhancement of the KCl concentration gradient in the present case is caused by the brine supersaturation required on the *hot* side of the droplet to make salt precipitate and the undersaturation on the *cold* side of the droplet needed to make salt dissolve. For the conditions of our experiment $J_D^{KCl} = 3.8 \times 10^{-9}$ moles KCl/cm²-sec.

Combining the basic salt and water conservation Equations (1) and (2) and Equation (3), we find that the velocity V of the vapor-liquid droplet is

$$V = \left(\frac{A_L}{A_G + A_L} \right) \left[\frac{C_L^{KCl}}{C_L^{H_2O}} \frac{A_G}{A_L} \frac{J_G^{H_2O}}{C_s^{KCl}} - J_D^{KCl} \right] \quad (10)$$

If $A_G/A_L \geq 7$, J_s^{KCl} may be neglected and the vapor-liquid droplet velocity V becomes

$$V = \left(\frac{A_G}{A_G + A_L} \right) \frac{C_L^{KCl}}{C_L^{H_2O}} \frac{J_G^{H_2O}}{C_s^{KCl}} \quad (11)$$

When the vapor phase in the vapor-liquid droplet contains a foreign gas in an amount sufficient to require diffusion transport of water in the vapor phase, then from Equation (5), the droplet velocity is

$$V = \frac{3}{2} \frac{C_L^{KCl}}{C_L^{H_2O}} \left(\frac{A_G}{A_L + A_G} \right) \frac{D_G^{H_2O}}{C_s^{KCl}} \frac{\partial C_G^{H_2O}}{\partial T} \nabla T_s \quad (12)$$

Foreign Gas in Vapor Phase.

The approximation $\Delta T_G \approx \frac{3}{2} \Delta T_s$ has been used since the thermal conductivity of both the gas and liquid are much less than that of the solid. Inserting typical droplet dimensions (see Table I) of $x = L = 15 \times 10^{-4}$ cm and $h = 1 \times 10^{-4}$ cm, we find that the velocity of a vapor-liquid droplet containing foreign gas in its vapor phase for the conditions of our experiment is 4.8×10^{-7} cm/sec in close agreement with our experimental measurements (see Table I). This agreement implies that our vapor-liquid droplets contained foreign gas in the vapor phase. The presence of foreign gas in our droplets was expected since the vapor-liquid droplets were formed at the free surface of the crystal, in contact with the atmosphere.

If the vapor phase in the vapor-liquid droplet contains only water vapor, then viscous gas flow will control the rate of H_2O transfer across the vapor phase. From Equation (4), the velocity of the vapor-liquid droplet is then,

$$V = \frac{3}{2} \left(\frac{A_G}{A_G + A_L} \right) \left(\frac{C_L^{KCl}}{C_s^{KCl}} \right) \left(\frac{C_G^{H_2O}}{C_L^{H_2O}} \right) \frac{(x-2h)^2}{25n_G^{H_2O}} \frac{\partial P_G^{H_2O}}{\partial T} \nabla T_s \quad (13)$$

No Foreign Gas in Vapor Phase.

Substituting in values of $x = 15 \times 10^{-4}$ cm and $h = 1 \times 10^{-4}$ cm, the vapor-liquid droplet velocity for the conditions of our experiment would be 4.6×10^{-4} cm/sec if the droplet contained no foreign gas.

APPLICATIONS TO THE STORAGE OF NUCLEAR WASTES IN SALT FORMATIONS

The thermomigration of liquid-brine droplets into nuclear waste burial crypts

Natural salt regularly contains about 0.4 atomic percent water in the form of small brine inclusions several hundred microns in diameter.⁽⁹⁾ In previous papers,^(16, 31) we have shown that such liquid-brine droplets will migrate up a temperature gradient towards higher tempera-

tures in salt. Thus brine droplets in a salt formation will be attracted to the heat generated by the self-heating of nuclear wastes in burial crypts. Over a limited temperature range, the velocity V' of sufficiently large brine droplets can be expressed as $V' = \beta \Delta T_s$, where β is a known constant (see Table II) and ΔT_s is the temperature gradient in the salt.^(16, 31, 32) For small brine droplets or low thermal gradients, this linear relation will not hold because of a kinetic barrier at the interface.⁽³¹⁾ The temperature gradient ΔT_s around a spherical burial crypt with a radius R_0 , that contains self-heating waste products at a temperature ΔT above the ambient temperature of the salt formation is,

$$\nabla T_s = - \frac{\nabla T R_0}{R^2}$$

where R is the radial distance into the salt formation. Consider a spherical shell of volume $4\pi R^2 dr$ surrounding the burial crypt. If dI is the inflow of water into the burial crypt (in moles of H_2O) generated by the thermomigration of brine droplets in this spherical shell, then

$$dI = \zeta 4\pi R^2 dr \quad (14)$$

where ζ is the density of liquid-brine droplets in the salt formation (in moles H_2O/cm^3). Inserting the relations $-dr = Vdt$, $V' = \beta \Delta T_s$, and $\Delta T_s = -\Delta T R_0/R^2$, we find the inflow of water per unit time dI/dt is

$$\frac{dI}{dt} = 4\pi \zeta \beta \Delta T R_0 \quad (15)$$

Substituting values of the constants listed in Table II ($\zeta = 1.08 \times 10^{-4}$ moles H_2O/cm^3 , $\beta = 5.9 \times 10^{-9}$ cm²/sec-°K, $\Delta T = 300^\circ C$, $R_0 = 100$ cm) for the NaCl- H_2O system, we estimate that the flow rate of water into the nuclear waste burial crypt will be 2.4×10^{-7} moles H_2O/sec . This is equivalent to an inflow of 140 cm³ of H_2O per year into the crypt. Recent results⁽³²⁾ from Project Salt Vault, a study of the actual storage of high-level nuclear wastes in a salt mine at Lyons, Kansas, show a water inflow into waste crypts of 365 cm³ per year, in reasonable agreement with our calculated value.

The transport of radioactivity away from the burial crypt by the thermomigration of biphasic vapor-liquid droplets

A further possible result of the self-heating of the nuclear wastes is that contaminated vapor-liquid biphasic droplets generated on the walls of the burial crypt may transport radioactive wastes away from the crypt into the salt formation. Such wastes could be carried in the vapor-liquid droplet as gases, liquids, dissolved solids or even as solid particles (Refs. 34-36). The velocity V of vapor-liquid droplets away from the burial crypt can be approximated in a limited temperature range as $V = -\alpha \Delta T_s$, where α is a known constant (see Table II). The time t

required for a vapor-liquid droplet to travel a distance R from the burial vault is

$$t = \int_{R_0}^R \frac{dr}{V}.$$

Substituting expressions for the velocity and the thermal gradient around a spherical waste crypt heated ΔT above the ambient temperature of the salt formation, we find that

$$R^3 - R_0^3 = (\alpha \Delta T R_0) t \quad (16)$$

where R_0 is again the radius of the burial crypt. Assuming that the self-heating of the nuclear wastes maintain the value at 300°C for the equivalent of two years, we find that vapor-liquid droplets containing a foreign gas could only transport radioactive wastes a distance of 10 cm into the salt formation. On the other hand, vapor-liquid droplets containing only water vapor in the vapor phase could carry nuclear wastes a distance of 600 cm into the salt formation in two years. This figure, however, ignores the pronounced ability of grain boundaries to trap migrating droplets.^(17, 18)

Escape of radioactivity to the external environment

Because the self-heating of the nuclear wastes will last only a relatively short time on a geological time scale, it is unlikely that thermal gradients generated by the self-heating wastes could cause thermomigration of contaminated liquid-vapor droplets out of the salt formation. On the other hand, both the permanent gravitational field⁽²⁹⁾ and the natural thermal gradient⁽¹⁶⁾ of the earth (2×10^{-4} °C/cm) could conceivably lead to the escape of fission waste products to the external environment. With an overlay of 100 meters of salt typical of the proposed Lyons, Kansas, nuclear waste burial facility, the calculated times required for a vapor-liquid droplet to escape from the salt formation because of the natural thermal gradient of the earth are 10^6 and 10^3 years, respectively, for vapor-liquid droplets with and without foreign gas in their vapor phase. These calculated times, however, again ignore the ability of grain boundaries to trap migrating droplets. Previous work has shown that fields significantly higher than either the gravitational field⁽¹⁸⁾ or the thermal gradient⁽¹⁷⁾ of the earth are necessary for a droplet to penetrate a grain boundary perpendicular to one of these force fields. Consequently, it appears that neither the gravitational field nor the thermal gradient of the earth could cause migration of contaminated droplets to the external environment even on a geological time scale.

SUMMARY

By considering viscous gas flow, vapor diffusion, liquid diffusion, evaporation-condensation, and liquid currents driven by surface tension gradients, the unusual ther-

momigration behavior of biphasic vapor-liquid droplets down thermal gradients in solids is explained. The thermomigration of these biphasic droplets and simple liquid droplets in natural salt formations was considered with regard to the proposed permanent storage of highly radioactive self-heating wastes in salt mines. It was concluded that an inflow of water into the nuclear waste crypts can be expected and that a modest dispersal of radioactive wastes into the salt formation may occur. However, because grain boundaries in salt can trap migrating droplets, it is unlikely that radioactivity will escape to the external environment even on a geological time scale.

REFERENCES

1. The National Academy of Science, *The Disposal of Radioactive Waste on Land*, National Research Council, Report of the Committee on Waste Disposal of the Division of Earth Sciences, Nat. Research Council Pub. 519, 412 (1957).
2. H. Krause, H. Ramdohr and M. C. Schuchardt *The Disposal of Radioactive Wastes Into the Ground*, p. 479, International Atomic Energy Agency, Vienna (1967).
3. H. Krause, H. Ramdohr, and G. Böhme, *ibid.*, p. 519 (1967).
4. R. L. Bradshaw, F. W. Empson, W. J. Boegly, Jr., H. Kubata, F. L. Parker, and E. G. Struxness, *Nucl. Struct. Eng.* 2, 4038 (1965).
5. W. J. Boegly, R. L. Bradshaw, F. M. Empson, and F. L. Parker, *Purdue Univ. Eng. Bull. Ext. Ser.* 106, 577 (1961).
6. F. L. Parker, W. J. Boegly, R. L. Bradshaw, F. M. Empson, L. Hemphill, E. G. Struxness, and T. Tamura, *Disposal of Radioactive Wastes*, Vol. 2, p. 365, Vienna, Int. Atomic Energy Agency (1960).
7. "A Nuclear Graveyard," *Newsweek*, March 29 edition, p. 60 (1971).
8. D. Farney, "Atomic Age Trash," *Wall St. Journal*, Jan. 25 edition, p. 1 (1971).
9. R. L. Bradshaw, F. M. Empson, W. J. Boegly, Jr., H. Kubota, F. L. Parker, and E. G. Struxness, *Geog. Soc. America Special Paper No. 88*, p. 643 (1968).
10. T. F. Lomenick and R. L. Bradshaw, *Nature* 207, 158 (1965).
11. J. Schechter and E. F. Gloyna, *Chem. Eng. Prog. Symposium Ser-Nuclear Eng., Ind. and Eng. Chem.* 55, 303 (1959).
12. W. R. Wilcox, *Ind. and Eng. Chem.* 60, 13 (1968).
13. W. R. Wilcox, *Ind. and Eng. Chem.* 61, 76 (1969).
14. E. Roedder, Kansas City Meeting, Geological Society America (1965).
15. E. Roedder, personal communication to W. R. Wilcox (1967).
16. T. R. Anthony and H. E. Cline, *Jour. Appl. Phys.* 42, 3380 (1971).

17. H. E. Cline and T. R. Anthony, *Acta Met* 19, 491 (1971).
18. T. R. Anthony and H. E. Cline, *Phil. Mag.* 23, 695 (1971).
19. H. E. Cline and T. R. Anthony, *Phil. Mag.* 24, 1483 (1971).
20. H. E. C. Powers, *Intern Sugar J.* 61, 17 (1959).
21. H. E. C. Powers, *Intern Sugar J.* 61, 41 (1959).
22. K. G. Denbigh and E. T. White, *Chem. Eng. Sci.* 21, 739 (1966).
23. E. Roedder, *Science* 155, 1413 (1967).
24. E. H. Kennard, *Kinetic Theory of Gases*, McGraw-Hill Book Co., Inc., New York (1938).
25. T. R. Anthony and R. A. Sigsbee, *Acta Met* 19, 1029 (1971).
26. V. G. Levich, *Physicochemical Hydrodynamics*, Prentice Hall Inc., Englewood Cliffs, N.J. (1962) p. 384.
27. A. V. Hershey, *Phys. Rev.* 56, 204 (1939).
28. Although γ/T is much larger than γ/C , the temperature effect on the vapor-liquid surface tension is swamped out by the concentration effect because the evaporation-condensation process produces a large concentration drop across the droplet while leaving unchanged the small temperature drop across the droplet.
29. T. R. Anthony and H. E. Cline, *Phil. Mag.* 22, 893 (1970).
30. H. E. Cline and T. R. Anthony, *Acta Met* 19, 175 (1971).
31. H. E. Cline and T. R. Anthony, *J. Appl. Phys* 43, 10 (1972).
32. W. C. McClain, R. L. Bradshaw, and F. M. Empson, *Disposal of Radioactive Wastes in the Ground*, p. 549, International Atomic Energy Commission, Vienna (1967).
33. P. Hoekstra, T. E. Osterkamp and W. F. Weeks, *J. Geophys. Res.* 70, 5035 (1965).
34. P. Hoekstra and R. D. Miller, U.S. Army Cold Regions Research and Engineering Laboratory, Res. Rpt. No. 153 (1965).
35. A. E. Corte, *J. Geophys. Res.* 67, 1085 (1962).
36. D. R. Uhlmann, Thesis, Harvard University (1963).
37. S. H. Maron and C. F. Prutton, *Principles of Physical Chemistry*, The Macmillan Co., New York (1959) p. 146.
38. I. J. O'Donnell and L. J. Gosting, *The Structure of Electrolytic Solutions*, W. J. Hamer, ed., John Wiley and Sons, Inc., New York (1959) p. 160.
39. L. G. Longworth, *J. Phys. Chem.* 61, 1557 (1957).
40. C. D. Hodgman, R. C. Weast and S. M. Selby, *Handbook of Chemistry and Physics*, Chemical Rubber Publishing Co., Cleveland (1958).
41. S. P. Clark, *Handbook of Physical Constants*, Geological Society of America Press, New York (1966).